

Polarization control and sensing with two-dimensional coupled photonic crystal microcavity arrays

Hatice Altug^{*} and Jelena Vučković[†]

Edward L. Ginzton Laboratory, Stanford University, Stanford, CA 94305-4088

Abstract

We have experimentally studied polarization properties of the two-dimensional coupled photonic crystal microcavity arrays and observed a strong polarization dependence of the reflection and transmission of light from the structure, as well as a strong polarization conversion. These effects can be employed in building miniaturized polarizing optical components and bio-chemical sensors. Our preliminary experimental results on chemical sensing with these structures are also presented.

OCIS codes: (230.0230) optical devices; (230.5440) polarization sensitive devices; (230.5750) resonators; (130.6010) Sensors

^{*} Also at the Department of Applied Physics, Stanford University, Stanford, CA 94305, altug@stanford.edu

[†] Also at the department of Electrical Engineering, Stanford University, Stanford, CA 94305, jela@stanford.edu, <http://www.stanford.edu/group/nqp>

We have recently proposed [1] and experimentally demonstrated [2] two-dimensional coupled photonic crystal resonator arrays (2D CPCRA), exhibiting a small group velocity over all wavevectors and in all crystal directions. These structures are interesting for construction of low-threshold devices such as photonic crystal (PhC) lasers with increased output powers and various nonlinear optical components. In our prior experimental work we measured the band diagram of such a structure by testing transmission through it at various incidence angles, thereby controlling the in-plane wavevector (k -vector); we demonstrated a small group velocity (below $0.008c$ at the Γ point) for a broad range of k -vectors [2]. In this article, we demonstrate a strong polarization sensitivity of CPCRA and their use both as chemical sensors and as miniaturized polarizing optical components.

When PhC microcavities are tiled in two dimensions thereby forming a 2D CPCRA (as shown in Fig. 1b), defect modes of individual cavities form coupled bands located inside the photonic bandgap of the surrounding photonic crystal. In particular, coupled arrays in the square PhC lattice exhibit three coupled bands: coupled monopole, dipole, and quadrupole [1-2]. Here we focus on the coupled dipole bands whose magnetic field components in the z -direction and at the center of the PhC slab are shown in Fig. 2a. Designed CPCRA were fabricated in silicon on insulator (SOI) by employing the procedure described in reference [2], and SEM pictures are shown in Fig. 1b. The size of the array is $100\mu\text{m}$ by $100\mu\text{m}$, and the PhC parameters are: the periodicity $a=488\text{ nm}$, the hole radius $r = 190\text{nm}$ and the slab thickness $d=275\text{ nm}$. The coupled cavities have two PhC layers between them in all directions and the unit cell size is $3a \times 3a$, as shown in the inset of Fig. 3. For this set of parameters, the Finite-Difference Time-Domain (FDTD) method predicts that the dipole mode is in the scanning range of our tunable laser (1460nm - 1580nm). Our experimental setup is shown in Fig. 1a. The structure is excited at the vertical incidence (in the z -direction, i.e., at the Γ point of the band diagram) by a tunable laser whose beam is linearly polarized in the x -direction and is slightly focused on the sample by using a very low numerical aperture (NA) objective lens. A total transmitted signal through the structure, as well as reflected signals of the same (x -direction) or opposite (y -direction) polarization are measured (the reflected signals are separated by employing a polarizing beam splitter in front of the top detector). The rotation of the structure around the z -axis is used to test the polarization dependence of the reflection and transmission. After the structure is rotated by an

angle ϕ around the z-axis, the excitation beam (the x-axis) is thus polarized in the direction ϕ of the structure, and the reflected signal of opposite polarization (the y-axis) then corresponds to a linearly polarized signal in the direction $\phi+90^\circ$ of the structure. The excitation of the high symmetry directions ΓX and ΓM hence corresponds to ϕ equal to 0° and 45° , respectively.

Fig. 2b shows the transmission spectra of the dipole bands at the Γ point; the red and blue curves are obtained for $\phi=0^\circ$ and $\phi=90^\circ$, respectively. Therefore, the red curve (with a resonance dip around 1564nm) corresponds to the excitation of the coupled x-dipole mode, and the blue curve (with a resonance dip around 1555nm) corresponds to the coupled y-dipole mode (see Fig. 2a for their field patterns). In a perfectly symmetric structure, the coupled dipole band has a double degeneracy at the Γ point, but splits into two sub-bands (x- and y-dipoles) away from the Γ point in the ΓX direction [1]. However, the results shown in Fig. 2b imply that the degeneracy of the dipole band in our structure is lifted at the Γ point, which is a result of the structural asymmetry under 90° rotation (the hole radius in the y-direction is roughly 5% larger than in the x-direction) [2].

In addition to the transmission through the structure, we have tested the reflected signal of opposite polarization relative to the incident signal, also at the vertical incidence (i.e., the incident signal is linearly polarized in the direction ϕ , and the reflected signal polarized in the direction $\phi+90^\circ$ of the structure is detected). The results for ϕ equal to 0° , 90° and 45° , corresponding to two different ΓX directions and the ΓM direction between them, respectively, are shown in Fig. 2c. Strong resonance peaks are observed at the locations of the coupled dipole bands; such peaks are not observed when the same experiment is performed on an unpatterned Si slab (without PhC). In the described experiment, we expect to observe only coupled x- or y-dipole modes, which are primarily polarized in the x- and y- directions, respectively. The x-dipole resonance at 1564nm has a higher quality (Q) factor and a narrower transmission linewidth than the y-dipole resonance at 1555 nm (Fig. 2a). For the incident light polarized in the $\phi=0^\circ$ direction, the x-dipole mode is primarily excited, and the reflected signal of opposite polarization ($\phi=90^\circ$) has only a small peak at the location of the coupled y-dipole band (Fig. 2c). Similarly, for the excitation polarized in the $\phi=90^\circ$

direction, the y-dipole is primarily excited, and the reflected signal with opposite polarization ($\phi=0^\circ$) exhibits a small peak at the location of the x-dipole band. On the other hand, for the excitation polarized in the ΓM direction ($\phi=45^\circ$), the reflected signal of opposite polarization exhibits a strong double-peak at the locations of the x-and y-dipoles, with a larger sub-peak at the x-dipole resonance, due to its higher Q-factor. In this case, the incident beam, which is linearly polarized in the $\phi=45^\circ$ direction, can be decomposed into two orthogonal components exciting both the x- and y-dipole modes, and the detected reflected signal in the $\phi=135^\circ$ direction is thus strong. Therefore, a CPCRA mixes up the polarization of the light coupled to it and acts as a polarization converter. In Fig. 3, we plot the polarization conversion, i.e., the amplitude of the measured reflected signal with opposite polarization as a function of the input polarization angle ϕ ; a cosine function (solid line) is fitted to experimental results (circles). The polarization conversion is maximum in the ΓM and minimum in the ΓX direction, as expected from the previous discussion. Similar type of oscillatory behavior in polarization conversion has been observed in elliptic metal nanohole arrays, but with broad polarization conversion peaks, resulting from losses in metals and low Q-factors of surface plasmon modes [3-4]. The advantage of PhCs relative to metallic nanohole arrays for this application is thus in minimization of non-radiative absorption losses and the ability to obtain a strong polarization conversion in a narrower wavelength range. For example, CPCRAs studied in this article have linewidths of about 7nm for the x-dipole mode; this is very close to the linewidth of the dipole mode in a single defect cavity, expected to be about 5nm, which indicates uniformity of the fabricated structures. By breaking the fourfold rotational symmetry of the structure further (i.e., by increasing the hole ellipticity), the two dipole modes can be separated even more in wavelength, thereby minimizing the polarization conversion in the ΓX direction. Such structures can be employed as polarizing mirrors: for a linearly polarized excitation in the ΓX direction, the transmission and reflection would exhibit a sharp dip and a sharp peak, respectively [5].

A strong reflected signal of opposite polarization (Fig. 2c) carries only information coming from photonic crystal, which eliminates the background signal and gives a very high signal to noise ratio. Moreover, its position is strongly dependent on the surrounding refractive index, which can be employed in bio-chemical sensing. Here we present our preliminary experimental results on chemical sensing. For this

purpose, we used another CPCRA with $a=467\text{nm}$, $r=195\text{nm}$ and $d=255\text{nm}$, in which the dipole modes are shifted to shorter wavelengths, so that they remain in the tunable range of the laser even after immersing the structure in a higher refractive index environment. The reference signal for $\phi=45^\circ$ excitation and for the structure in air is shown in Fig. 4b. Dipole band splitting resulting from the hole ellipticity can be observed again, with the y and x-dipole resonances at 1525nm and 1536nm , respectively (in this case, the Q-factor of the y-dipole is higher). The chemical sensing experiment is performed by dropping a small amount of isopropanol (IPA, refractive index $n=1.377$) and methanol ($n=1.328$) separately on the same structure. The reflected signal of opposite polarization for the structure covered with IPA is shown in Fig 4c: the spectrum is clearly shifted to longer wavelengths, as expected, but the two peaks are now equally strong and more separated. This is a result of the method employed in this measurement: the liquid drop forms a lens like shape on the structure, which refracts the incident light, leads to non-zero k-components and a spread in ϕ ; this, in turn, excites strongly both x- and y- dipoles in a range of k-vectors away from the Γ point, where the two bands are strongly nondegenerate. This problem would not be present if the liquid covered the structure uniformly, which would be possible by integrating microfluidic channels with PhC. The reflection spectrum from the same structure for methanol is very similar to IPA, again with two peaks, but at shorter wavelengths relative to IPA, as expected. We have estimated the wavelength shift theoretically by the FDTD method for the same structure without any hole ellipticity (i.e., with degenerate dipole modes at the Γ point). Since the size of the droplet (around 5mm by 5mm) is large compared to the structure, we have assumed in the simulation that the liquid completely surrounds the structure and penetrates holes. Fig. 4a shows the resonance wavelength shift as a function of the surrounding refractive index, and a very good agreement between theory and experiment can be observed (the two experimental lines correspond to the x- and y-dipoles). By immersing the structure into IPA instead of methanol, the refractive index changes by $\Delta n = 0.049$, and the dipole band position shifts by $\Delta\lambda = 7\text{nm}$. A similar sensitivity has been observed recently in a single PhC cavity based sensor in the passive configuration [6], but a CPCRA sensor has the following advantages: a better signal to noise ratio (as a result of the detection of the reflected signal with opposite polarization) and a simpler positioning of the analyzed material (since the cavities are distributed over a larger area). The sensitivity can be improved by changing the type of cavities inside CPCRA (e.g., by reducing hole diameters periodically, instead of completely removing them, such that the overlap

between the field and a reagent is stronger), or by embedding an active quantum well layer inside the structure and using it above lasing threshold, where the linewidth narrows [7]. Finally, since the coupled bands are flat, a CPCRA sensor would have a high sensitivity at different incidence angles, meaning that it can be alignment tolerant.

In conclusion, we have experimentally analyzed strong polarization properties of 2D CPCRA. The reflected signal with opposite polarization relative to the excitation exhibits strong resonance peaks (with a very large signal to noise ratio) at the locations of the coupled bands. Such polarization conversion (strongest in the Γ M direction) can be employed in building miniaturized polarizing optical components. Moreover, by breaking the rotational symmetry, such structures can also be employed as polarizing mirrors. All of these properties can be tuned by structural modifications. Finally, we have also experimentally demonstrated that coupled resonator arrays can be used as high sensitivity, high signal-to noise ratio, and alignment-tolerant chemical sensors that can be easily integrated with microfluidics.

Acknowledgment: This work has been supported by the Marco Interconnect Focus Center Research Program, and in part by the MURI Center for Photonic Quantum Information Systems (ARO/ARDA program DAAD19-03-1-0199), the Charles Lee Powell Foundation Faculty Award and the Terman Award.

References:

- [1] H. Altug, J. Vučković, Appl. Phys. Lett. **84**, 161 (2004)
- [2] H. Altug, J. Vučković submitted for publication. (<http://www.arxiv.org/abs/physics/0406109>)
- [3] R. Elliott, I. I. Smolyaninov, N. I. Zheludev, A. V. Zayats, Opt. Lett. **29**, 1414 (2004)
- [4] R. Gordon, A. G. Rajora, B. Leathem, K. L. Kavanagh, Phys. Rev. Lett. **92**, 037401-1 (2004)
- [5] We have recently learned that another group theoretically analyzed polarizing mirrors based on square PhC lattices with broken fourfold rotational symmetry: V. Lousse, W. Suh, O. Kilic, S. Kim, O. Solgaard, S. Fan, Opt. Express, **12**, 1575 (2004)
- [6] E. Chow, A. Grot, L. W. Mirkarimi, M. Sigalas, G. Girolami, Opt. Lett. **29**, 1093 (2004)
- [7] M. Loncar, A. Scherer, Y. Qiu, Appl. Phys. Lett. **82**, 4648 (2003)

Figure Captions:

Figure 1. (a) Experimental setup used in measurement of the CPCRA band diagram. The explanation of symbols is as follows: $\lambda/2$ - half-wave plate, BS – non-polarizing beam splitter, PBS - polarizing beam splitter, OL - objective lens, IR-cam - infrared camera and D – detector. Rotation of the structure around the z- axis is controlled by a rotation stage. (b) SEM pictures of the fabricated CPCRA with $A=3a$.

Figure 2. (a) Magnetic field (B_z) patterns of the coupled dipole bands at the Γ point (b) Transmission spectra of the CPCRA for the coupled x- (red, $\phi=0^\circ$) and y- (blue, $\phi=90^\circ$) dipole modes at the Γ point. (c) Reflection spectra of the CPCRA at the opposite polarization relative to the excitation, for $\phi=0^\circ$, 45° and 90° respectively. In the $\phi=0^\circ$ ($\phi=90^\circ$) case, the x- (y-) dipole band is primarily excited, so a small peak shown here corresponds to the weak excitation of the y- (x-) dipole band. In the $\phi=45^\circ$ case, both dipole bands are equally excited, and a strong polarization conversion is observed.

Figure 3. Polarization conversion, i.e., the amplitude of the reflected signal with opposite polarization relative to the excitation as a function of the input polarization angle ϕ (circles). The solid line is a cosine function fit to the experimental data. (Both experimental data and a fit are normalized by the maximum value of this cosine fit). The inset shows a unit cell of CPCRA with $A=3a$ and high symmetry directions.

Figure 4 (a) The resonance wavelength as a function of the surrounding refractive index. The three data points correspond to the structure in air ($n=1$), methanol ($n=1.328$) and IPA ($n=1.377$). Triangles and stars correspond to the wavelength shifts of the y-dipole and x-dipoles respectively, and circles show the wavelength shift simulated by FDTD for the same structure without any hole ellipticity. Lines are fitted to experimental data points. (b) The reflection spectrum with opposite polarization with respect to the excitation for the structure in air. Arrows indicate the positions of the x- and y- dipole bands (c) The same spectrum when the structure is immersed in IPA.

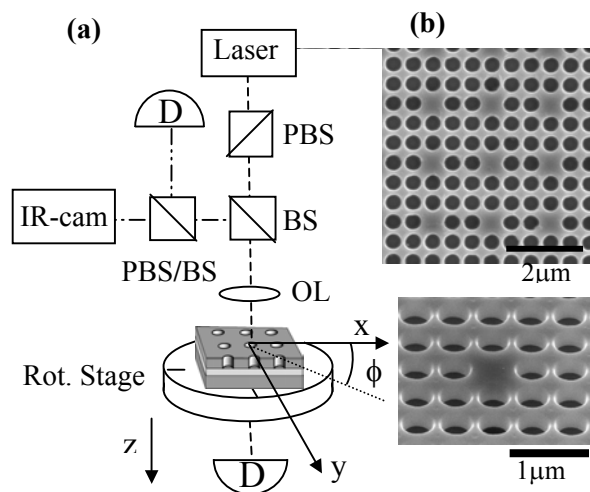


Figure 1

Authors: H. Altug, J. Vuckovic

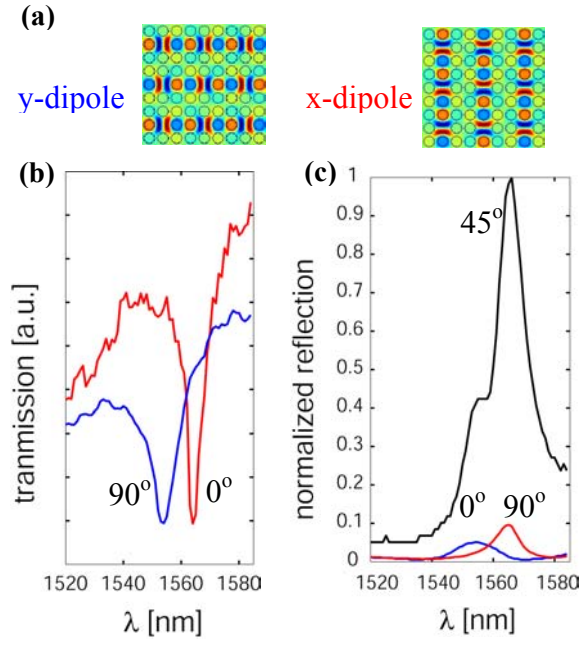


Figure 2

Authors: H. Altug, J. Vuckovic

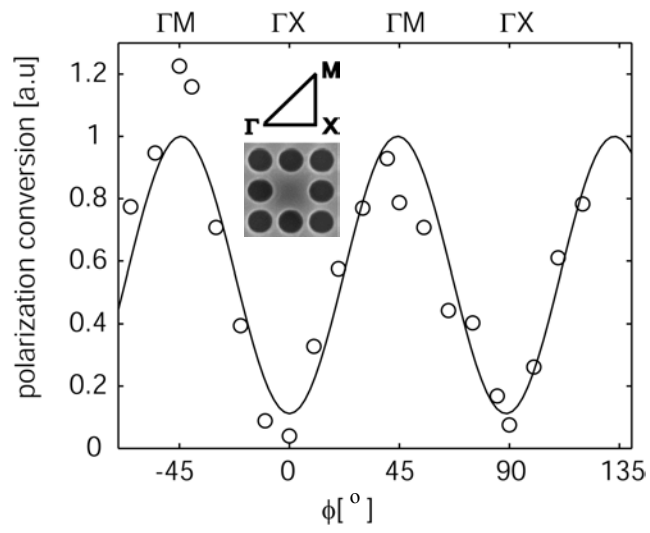


Figure 3

Authors: H. Altug, J. Vuckovic

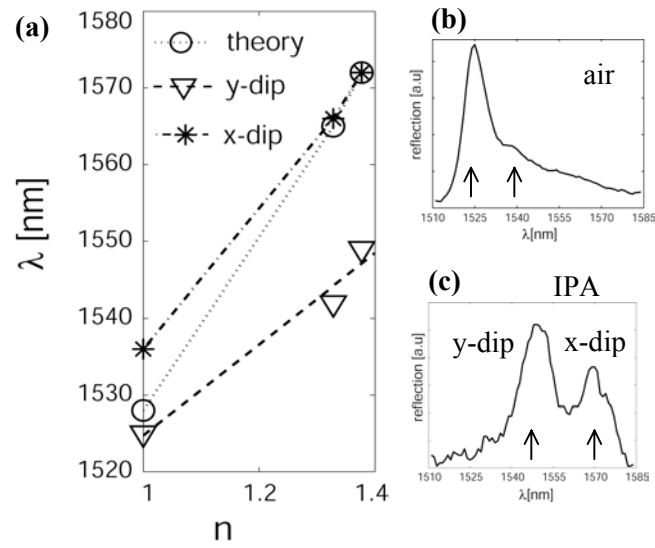


Figure 4

Authors: H. Altug, J. Vuckovic